Spectrophotometric calibration of the Swope and DuPont Telescopes for the Carnegie Supernova Project 2.

J.-P. Rheault*, Nicholas. P. Mondrik, D. L. DePoy, J. L. Marshall, Nicholas B. Suntzeff,
Department of Physics and Astronomy, Texas A&M University, 4242 TAMU, College Station, TX 77843

ABSTRACT

We present results from the spectrophotometric calibration of the new E2V CCD camera on the Swope telescope and of RetroCam on the DuPont Telescope. We measured the relative sensitivity of each pixel vs wavelength over the whole wavelength sensitivity range of each camera, for all the filters that will be used during the 5 years of the CSP2 survey. We used a tunable light source and fiber delivery system conceived and built in our lab to achieve +/-1% precision calibration from 300nm to 1100nm and +/-3% from 1100nm to 1800nm. Achieving this relatively high precision at low light levels was made possible by using Si, Ge and InGaAs photodiodes coupled to custom high gain amplifiers. Comparison of these results to results obtained 3 years before, allowed us to confirm that the intrinsic transmission bandpass of the filters has not changed over time but that the mirror reflectivity and the introduction of a new CCD camera drastically changed the total telescope sensitivity. The analysis of the spatial response of the new E2V CCD vs wavelength also shows a slight gradient in the color response of the CCD both in the UV and Infrared.

Keywords: instrumentation, detector, CSP, calibration, photometry

1. INTRODUCTION

Current and future generations of large scale cosmological surveys will rely heavily on precise calibration of the astronomical datasets to produce precision results. Surveys such as PanStarrs [1], LSST [2], and the Dark Energy Survey[3] (DES), and others like them, will produce data that are capable of making high precision cosmological measurements made possible in part by photometric datasets that are accurate to better than 0.01 magnitude, but only when properly calibrated. Carefully constructed calibration systems are being planned, constructed, and tested for these surveys[4, 5, 6].

The Carnegie Supernova Project II (CSP2) is one such survey that aims at achieving very high precision photometry. It is a five-year program that will obtain optical and near-infrared observations of 100-150 Type Ia supernovae located in the smooth Hubble flow. The main emphasis is to obtain near-infrared light curves and time-series spectroscopy in order to achieve a distance precision of 1-2%, as well as to build a definitive low-redshift reference for future rest-frame infrared observations of distant Type Ia supernovae. The ambitious distance precision requires a well calibrated filter response curve and the certainty that the response is stable over the duration of the survey.

In this paper, we present the results from the bandpasses transmission calibration from 300nm to 1800nm performed in October and November 2013 at the Las Campanas Observatory in Chile. The instrument used for this calibration is similar to the DECal instrument permanently installed on the DECam camera at CTIO[4]. Other groups[5] have used tunable laser based instruments to perform similar work in the wavelength range from 300nm to 1100nm. Our current instrument has the unique capability of performing spectrophotometric calibrations at wavelengths up to 1800nm. This allows us to characterize the Y, J and H band of the CSP survey.

In section 2 we will give a brief description of the experimental setup. In section 3 we will present our transmission measurements and compare with results from similar measurement performed 3 years earlier for the first CSP survey[7] to evaluate long term stability of the filter band passes. Section 4 will detail the error budget. Finally, section 5 will present an analysis of the spatial dependence of our filter transmission measurements where we will focus mainly on the color dependence of the E2V CCD sensitivity and of the filter response.

*jprheault@physics.tamu.edu

2. EXPERIMENTAL SETUP

2.1 General description

A schematic of the experimental setup is shown in figure 1. The experimental setup consists of a broadband light source from which we select a narrow bandwidth (~1-2 nm FWHM below 800nm, 10nm FWHM above 800nm) using a monochromator. The monochromator output is coupled into a fiber bundle made of 11 fibers aligned in a single row. The fiber bundle brings the light to the top of the telescope, behind the secondary mirror. Light is projected onto the flat field screen from the center of the telescope axis with beam projection optics that ensures uniform illumination of the screen. Silicon, Germanium and InGaAs NIST traceable calibrated photodiodes, also placed behind the telescope secondary mirror, measure the power on the screen. A sample of the illumination beam is fed to a spectrometer that monitors in real time the illumination wavelength with an accuracy of ~0.3nm. For more information on the experimental setup please refer to our previous SPIE papers[5, 6]

2.2 Light source:

We used 2 light sources to cover the wavelength range from 300nm to 1600nm.

1. 75W Xenon arc lamp, used from 300nm to 800nm. The presence of strong emission lines in the spectra beyond 800 nm prevents us from using this light source there.
2. 250W quartz tungsten halogen lamp, used from 800nm to 2000nm. This light source is not as bright so the light throughput at the screen is about 5 times less than the Xenon lamp.

2.3 Monochromator:

A monochromator was used to select a narrow bandwidth from the source. In order to optimize throughput we used a variety of light sources, grating and slit widths during the calibration. The following table shows a summary of the operating conditions for each filter scan.

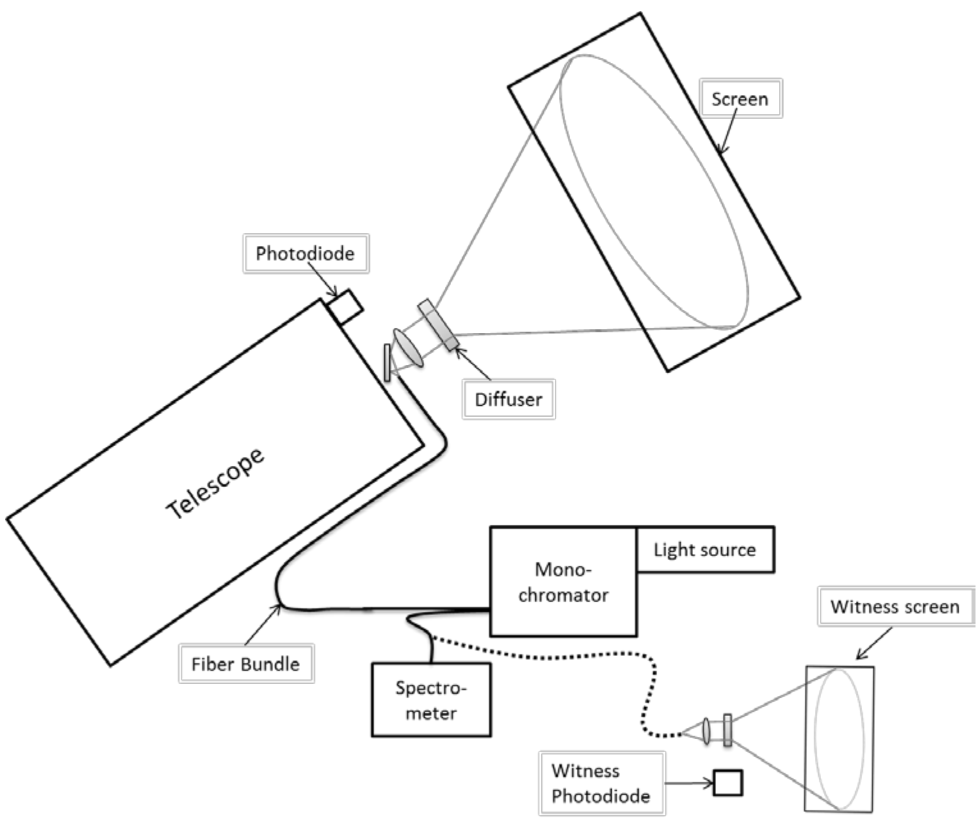

Figure 1: Experimental setup

Monochromator parameters for Swope (UV-Visible)							
Filter	u	B	V	g	r	i	no filter
Wavelength range	300-600	300-600	400-800	300-600	400-800	600-1000	300-1000
Order sorting filter	295	295	400	295	400	595	295, 400, 595
Light FWHM	2.5 nm	2.5 nm	2.5 nm	2.5 nm	2.5 nm	4 nm	10 nm
Input slit width	0.78 mm	0.78 mm	0.78 mm	0.78 mm	0.78 mm	2.2 mm	0.78 mm
Output slit width	Fully open	Fully open	Fully open	Fully open	Fully open	Fully open	Fully open
Grating	400 nm blaze, 1200 l/mm	400 nm blaze, 1200 l/mm	750 nm blaze, 1200 l/mm	400 nm blaze, 1200 l/mm	750 nm blaze, 1200 l/mm	750 nm blaze, 1200 l/mm	400 and 750 nm blaze, 1200 l/mm and 1250nm blaze, 600 l/mm
Light source	Xenon	Xenon	Xenon	Xenon	Xenon	Xenon and Quartz	Xenon and Quartz
Integration time	60s and 120s	60s	60s	60s	60s	60s	60s
Photodiode	Si	Si	Si	Si	Si	Si	Si

Table 1: Monochromator parameters for Swope (UV-Vis)

Monochromator parameters for DuPont (Infrared)			
Filter	Y	J	H
Wavelength range	900-1200	1000-1450	1400-1900
Order sorting filter	695	695	1000
Light FWHM	10 nm	10 nm	10 nm
Input slit width	2 mm	2 mm	2 mm
Output slit width	Fully open	Fully open	Fully open
Grating	1250 nm blaze, 600 l/mm	1250 nm blaze, 600 l/mm	1250 nm blaze, 600 l/mm
Light source	Quartz	Quartz	Quartz
Integration time	30s, 50s and 200s	50s and 200s	50s and 250s
Photodiode	Ge	InGaAs	InGaAs

Table 2: Monochromator parameters for DuPont (Infrared)

2.4 Wavelength calibration

Having an accurate wavelength measurement is crucial in the case of filters with sharp edges. Since the monochromator wavelength selection accuracy is 1nm, we designed our fiber bundle to have an extra fiber that samples the power at the output slit and feeds it to a spectrometer. Our spectrometer was calibrated using Mercury, Argon and Neon calibration lamps. We believe our wavelength accuracy is better than 0.2nm.

In the infrared, we did not measure directly the wavelength with the spectrometer so our wavelength uncertainty is about 1nm. The main reason is that our spectrometer has a maximum wavelength range of about 1000nm. This increased error on the wavelength is acceptable since the FWHM of the light is 10nm in the infrared.

2.5 Data acquisition

For each filter, we monitor the light entering the telescope by measuring the light reflected off the dome flat screen with photodiodes placed behind the secondary, facing the screen. The signal from these photodiodes was measured by a multi channel analog to digital card with an acquisition rate of 1kHz per channel. We averaged data every 0.25s to and saved both the 1kHz and 0.25 Hz data in a file.

2.6 Detectors:

We used 3 different types of detectors for this calibration:

Detector type	Wavelength range	Detector size	Calibration	Pointing
Silicon	300 to 900nm	10x10mm	Our lab, NIST traceable	Dome flat screen
Germanium	900nm to 1100nm	10mm dia	Our lab, NIST traceable	Witness screen
InGaAs	1100nm to 2400nm	2mm dia	National research council of Canada (NRC)	Witness screen

Table 3: Detectors used during calibration

The Germanium (Ge) and Silicon (Si) detectors were calibrated in our lab using an NIST traceable Gentec calibrated photodiode. Even if the Ge detector sensitivity extends from 900 to 1600nm, we used the InGaAs photodiode, directly calibrated by the NRC, when available (above 1100nm) for better precision.

2.7 Witness screen (For DuPont only)

Due to the lower light levels produced by our system in the infrared and because of the reduced sensitivity of the InGaAs detector caused by the smaller surface area, we had to use a witness screen to increase the signal at the InGaAs detector. The witness screen was illuminated using the central fiber that bifurcates from the fiber bundle and was used to monitor the wavelength in the visible (See figure 1). Instead of sending the light into the spectrometer, we projected it on a small (35x35cm) screen made of the same material as the Dome Flat Screen (Duraflect). We then placed the InGaAs detector and one of the Ge detectors about 10cm from the witness screen. The signal read from the witness screen is about 50 to 500 times stronger than what is seen from the big screen since the photodiodes are much closer to the witness screen. Care was taken to ensure that the optical paths in both the witness screen and the dome flat screen were identical: same fiber length, same projection optics, same white reflective material. Figure 2 shows that the relative signal measured simultaneously by 2 Ge detectors at the 2 screens is identical within measurement errors. Based on that observation, we are confident that we can use the witness screen for the InGaAs detector.

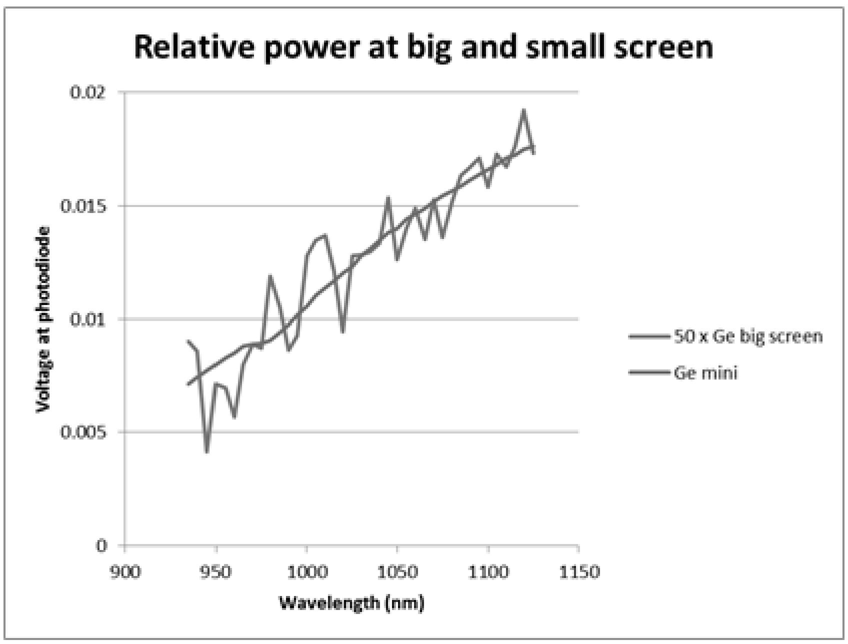

Figure 2 relative power between witness and dome flat screen

2.8 Thermal drift

A challenge inherent with IR measurements is the presence of relatively important and fast background thermal drifts. To minimize this problem, we took the data using the following method.

Camera background removal
For each wavelength, we took a “Dark” image and “Light” images of the same duration. (A “Dark” image is taken with the light off and a “Light” image is taken with the light on.) We subtract the dark from the light to get a measurement. In addition, since RetroCam exhibited image persistence, we took a short (6s) dark exposure after each light exposure to “clear” the camera detector.

Detector drift correction
The photodiode detectors are not temperature stabilized so the amplifiers and background drift significantly during the ~60 second exposure time but is relatively stable on a 1s time scale. The error caused by the drift is much more important than the noise on the detector. It is then better to take shorter integration times (~1 second) to avoid drift problems even if we sacrifice a bit of averaging of the noise.
Since the output of the lamp is very stable (<1% over a period of hours), we decided to assume that the output was constant over the 30s exposure time and only measure the amplitude just before opening the shutter to take a camera image. Before each exposure, we cycle the light shutter on and off 5 times for a 10 second period and get 5 values of the amplitude that we average to calculate the power at the detector. (See figures 3a and b)

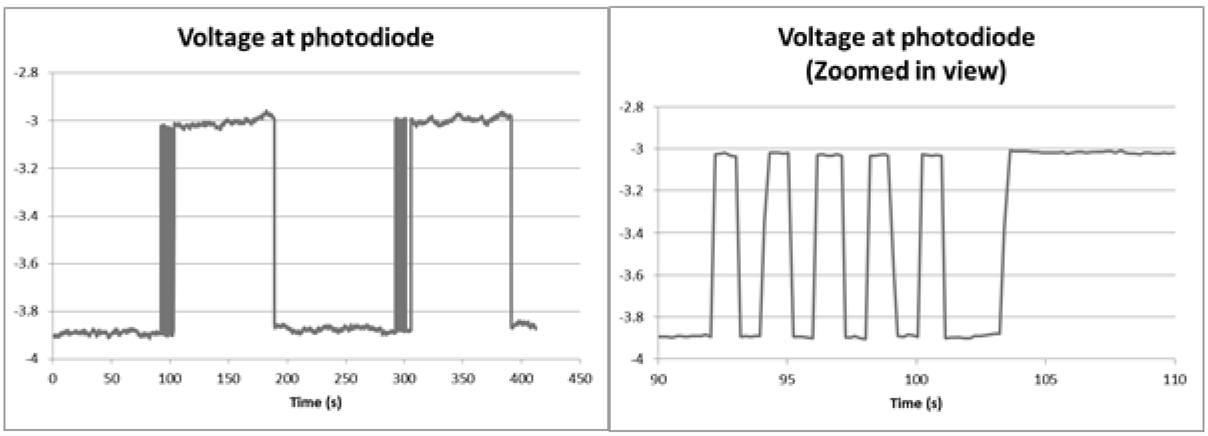

Figure 3a and 3b: Voltage at photodiode

3. MEASURED FILTER TRANSMISSION

In this section we present the measured transmission functions for both the E2V CCD on the Swope (Figure 4a) and RetroCam on DuPont (Figure 4b) that were measured in Fall of 2013, just before the start of the CSP2 survey.

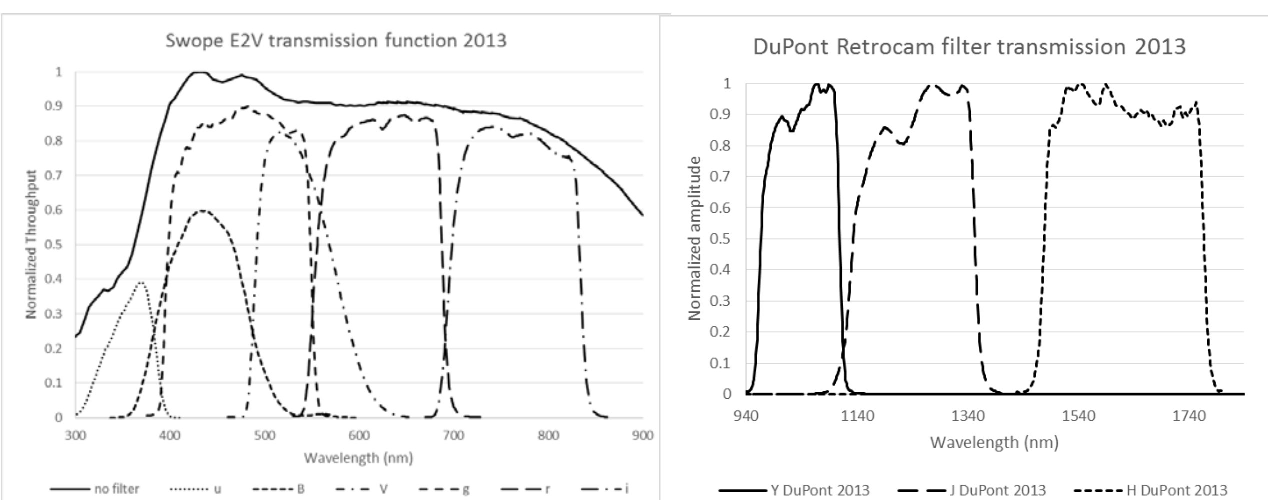

Figure 4a and 4b: Transmission function for the Swope and DuPont telescopes

The Swope measurements show the relative transmission of the each of the filters and of the telescope without filters in the beam path. The DuPont data shows the transmission for the 3 filters that were measured. We could not measure the system transmission without filters on the DuPont telescope since the RetroCam camera did not have an "open" position on the filter wheel.

For reference we also show the same measurements performed 3 years ago on the same telescopes. Following up after 3 years allows us to verify several things. First, since CSP2 uses a new CCD that was not used with the first CSP, we can calculate the correction we need to apply to the photometry because of the different response vs wavelength of this new CCD. Second, we can verify that the intrinsic filter transmission has not changed or degraded with time. Third, for the measurements that remain the same over the 3 year period, we can validate the accuracy of our measurement system.

3.1 u, B, V, g, r, i change from Jan 2010

Figure 5 shows the change in transmission of the CSP bandpasses for the Swope from 2010 to 2013. Since our measurements doesn't allow us to measure the absolute transmission. We have normalized both series of data so that the maximum transmission of the system without filter is 1. A quick visual inspection of the "No Filter" curves shows that the E2V CCD (2013) has a flatter response than the old SITE#3 CCD (2010). This difference in CCD response vs wavelength is the main driver of the change of the transmission response for the filters. We measured the intrinsic filter transmission on an optical bench and confirmed that there was no change in the during the 3 year period within experimental error.

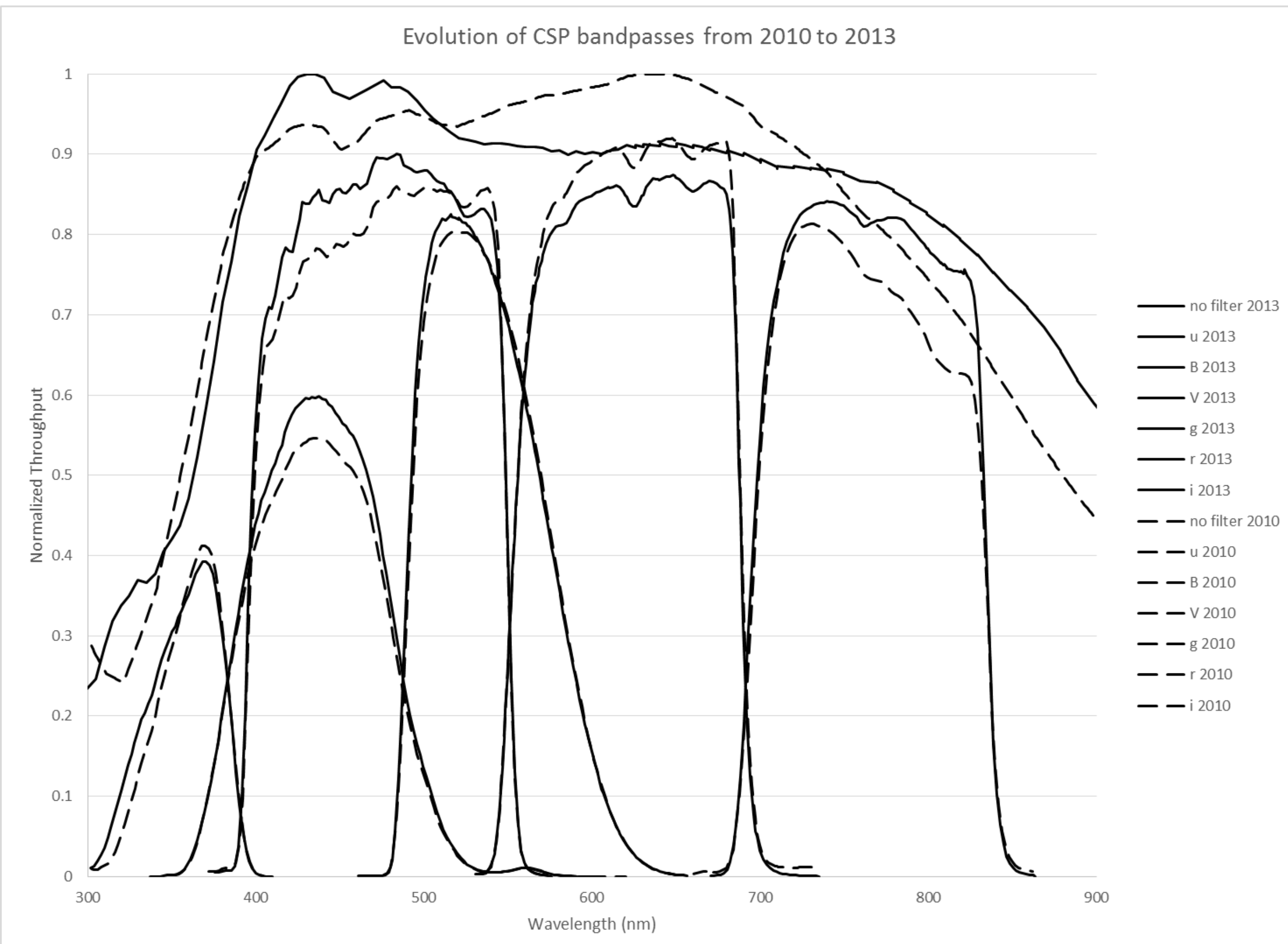

Figure 5: Evolution of CSP bandpasses from 2010 to 2013 for the Swope Telescope.

3.2 Y, J, H change from Jan 2010

Figure 6 shows the change in the transmission function of the infrared bandpasses between when the RetroCam camera was on the Swope in 2010 and when it was moved to the Dupont in 2013. Both set of measurements were normalized before the comparison. The transmission function has not changed much between the measurements. In all cases, the filter edges have not shifted in wavelength. The biggest difference is in the H filter and is likely due to a difference in reflectivity of the Swope and DuPont mirrors. One thing to keep in mind is that our experiment doesn't allow us to measure an absolute transmission so a direct comparison of the amplitude of the 2010 and 2013 data is not possible. One should use standard stars to compare the absolute throughput of each filters.

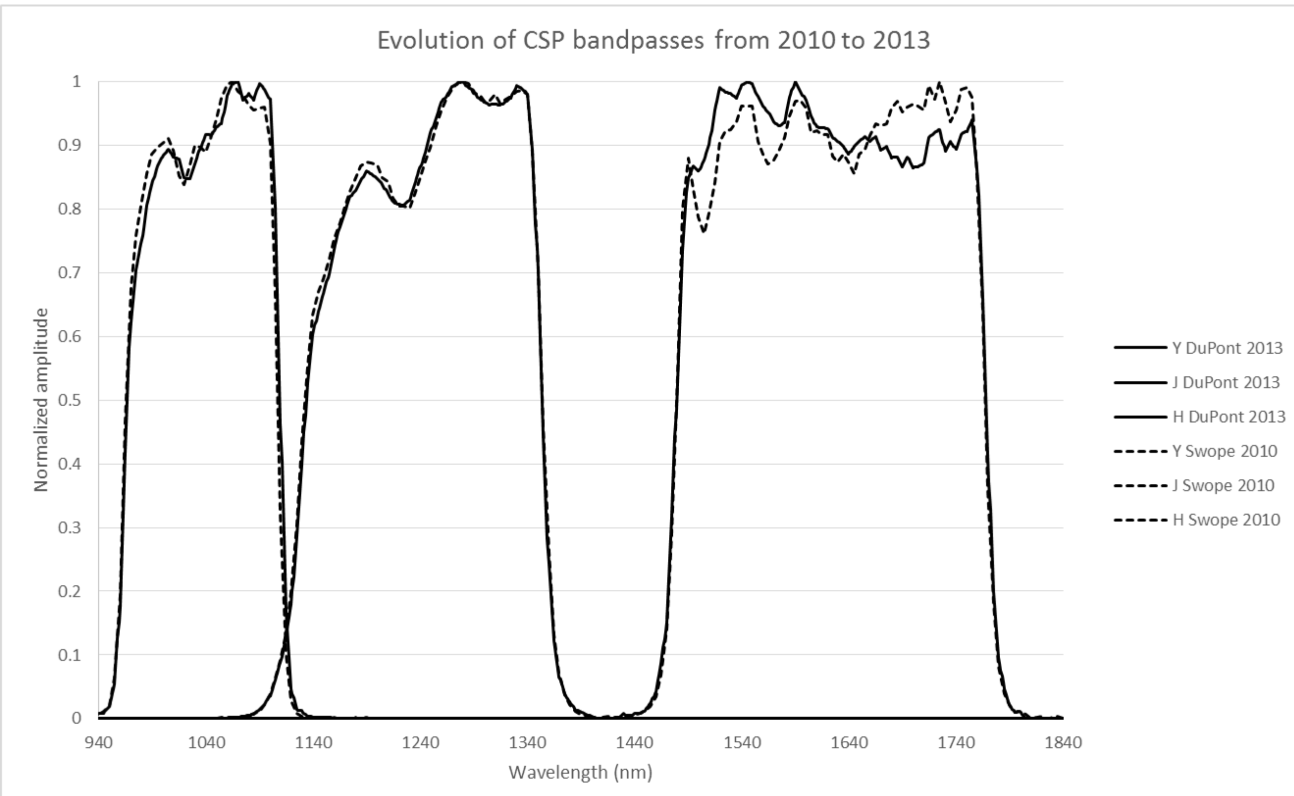

Figure 6: Evolution of CSP bandpasses from 2010 to 2013 for RetroCam

4. E2V CCD SPATIAL AND COLOR DEPENDENCE ANALYSIS

The second installment of the Carnegie Supernova Project will benefit from a significant upgrade of the camera used in the UV-Vis. One of our goal in measuring the throughput of this new camera is to detect and possibly correct or mitigate any spatial color dependence of the new CCD. The new E2V CCD is a significant upgrade from the SITE #3 CCD that was used during the original CSP survey. The CCD readout time is faster and the CCD size is bigger. The bigger size means that it is more susceptible to vigneting, especially from the filters. We know that the sensitivity of the CCD is not perfectly uniform vs wavelength so to compensate for that, we wanted to find the best location on the CCD to position the science targets to get the most repeatable results. Our results indicate that the middle of the third quadrant (Q3) is the position on the CCD that has the most uniform response.
All the results presented in the previous section were values measured at that specific location (Center of Q3) on the E2V CCD that will be used during the survey. The results were calculated at each wavelength step by using the median value of a 500 by 500 pixel box centered in quadrant #3 of the CCD [774:1274,774:1274].
We now propose to study the spatial response of the whole CCD. To do so, we subdivide the whole CCD into 6 regions.

1- Amplifier 1 (upper right): [2349:3796,2349:3796]
2- Amplifier 2 (upper left): [300:1748,2349:3796]
3- Amplifier 3 (lower left): [300:1748,300:1748]
4- Amplifier 4 (Lower right): [2349:3796,300:1748]
5- All: pixels in the range [300:3796,300:3796]
6- Center: pixels in the central region [1348:2749,1348:2749]

We will use the median value of all pixels in the CCD (region 5) as a baseline for our calculations The first 4 regions are the 4 different amplifiers, the 5th region is ALL pixels and the 6th region is a sub region in the center.
To try to illustrate how the sensitivity of the CCD changes vs pixel position and wavelength, we present two plots obtained with our measurements. The first one studies the response without filter and the second, the response with the r filter. In each plot, for each individual wavelength, we divide the median CCD counts in the selected region by the median CCD counts in the whole CCD (Excluding a narrow row of 300 pixels on the edge of the CCD that are affected by obvious vignetting or edge effects)

4.1 No Filter

The first plot shows the response of the telescope + CCD without filters. We can see that region 1 (upper right quadrant) is less sensitive at all wavelength when compared with all pixels and that region 3 (lower left quadrant) is more sensitive. That is not a problem and is probably due to different gains in the amplifiers. It can easily be taken out by flatfielding. Unfortunately, there is also a color dependent difference between the different regions, especially below 400nm, where region 1 is significantly less sensitive (4%) than the average and section 2 is more sensitive by 4%. In the infrared, (above 800nm) region 1 is also less sensitive than average. That color dependent term is a potential problem since it cannot be corrected using a flatfield.

One way to mitigate the color dependence of the focal plane is to confine all the science objects to a small region of the CCD. When we zoom into the smaller, 500x500 pixel box that will be used for the CSP data (filled circles), the uniformity improves drastically and the sensitivity is flat vs wavelength to a fraction of 1%.

To further illustrate the color dependence of the CCD response, Figure 8 also shows an image of the CCD response with “No Filter” at 350nm. We can see that there is a diamond pattern at a level of +/-1% that is caused by the manufacturing process. The large scale gradient has an amplitude of 4% and is what we see on the spatial dependence graph. The center of Q3 (Lower left quadrant) sits in a saddle point in the non-uniformity and is thus less affected by the color dependence.

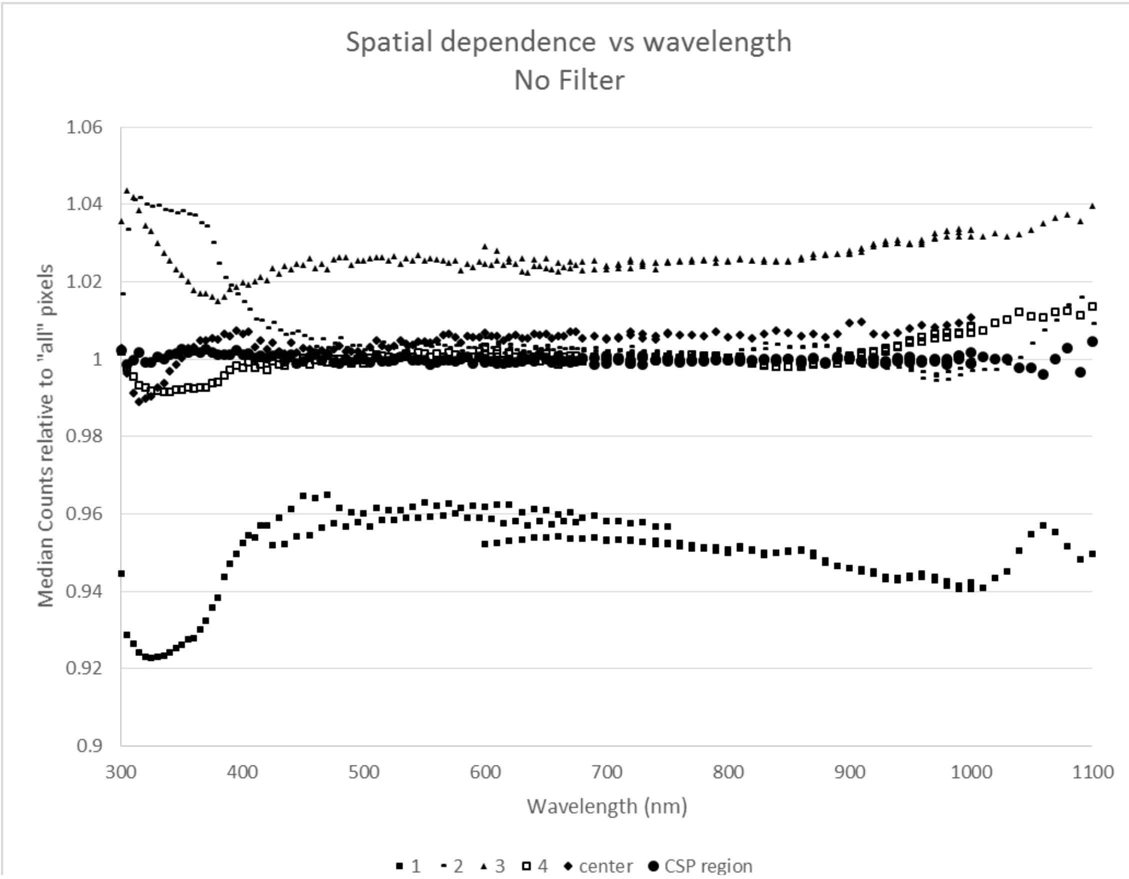

Figure 7: Spatial dependence vs. Wavelength for no filter

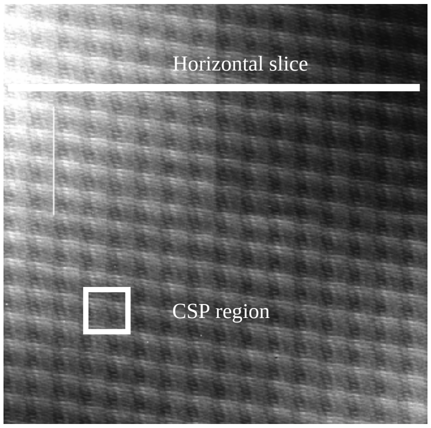

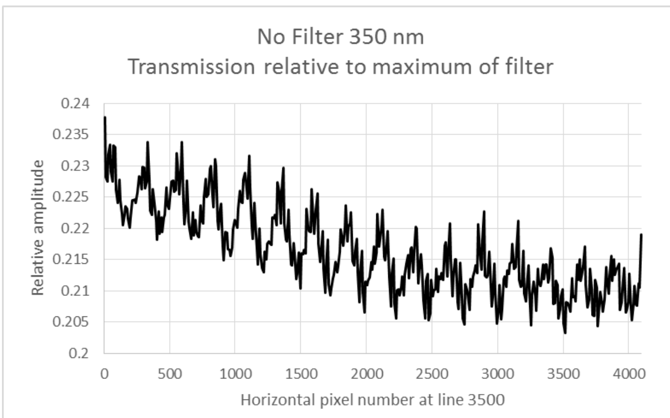

Figure 8a and 8b: (Left) CCD image at 350 nm with no filter, (Right) horizontal slice of the image at line 3500.

4.2 r Filter

The main source of spatial dependence vs wavelength of filters is at the edge of the filters, when the transmission of the filters changes rapidly vs wavelength. In these wavelength ranges a small change in wavelength results in a very large change in transmission. Figure 9 below illustrates this effect well. The response of the CCD is very flat vs wavelength in the high transmission wavelength range of the filter for all positions on the filter but at the filter cut-on and cut-off wavelengths, the relative filter transmission changes significantly between the different regions. Figure 10a shows the CCD image taken at 694 nm, where the filter transmission has fallen to ~15%. We can see a circular gradient that is centered on the optical axis of the telescope that is due to an uneven response of the filter at different positions.

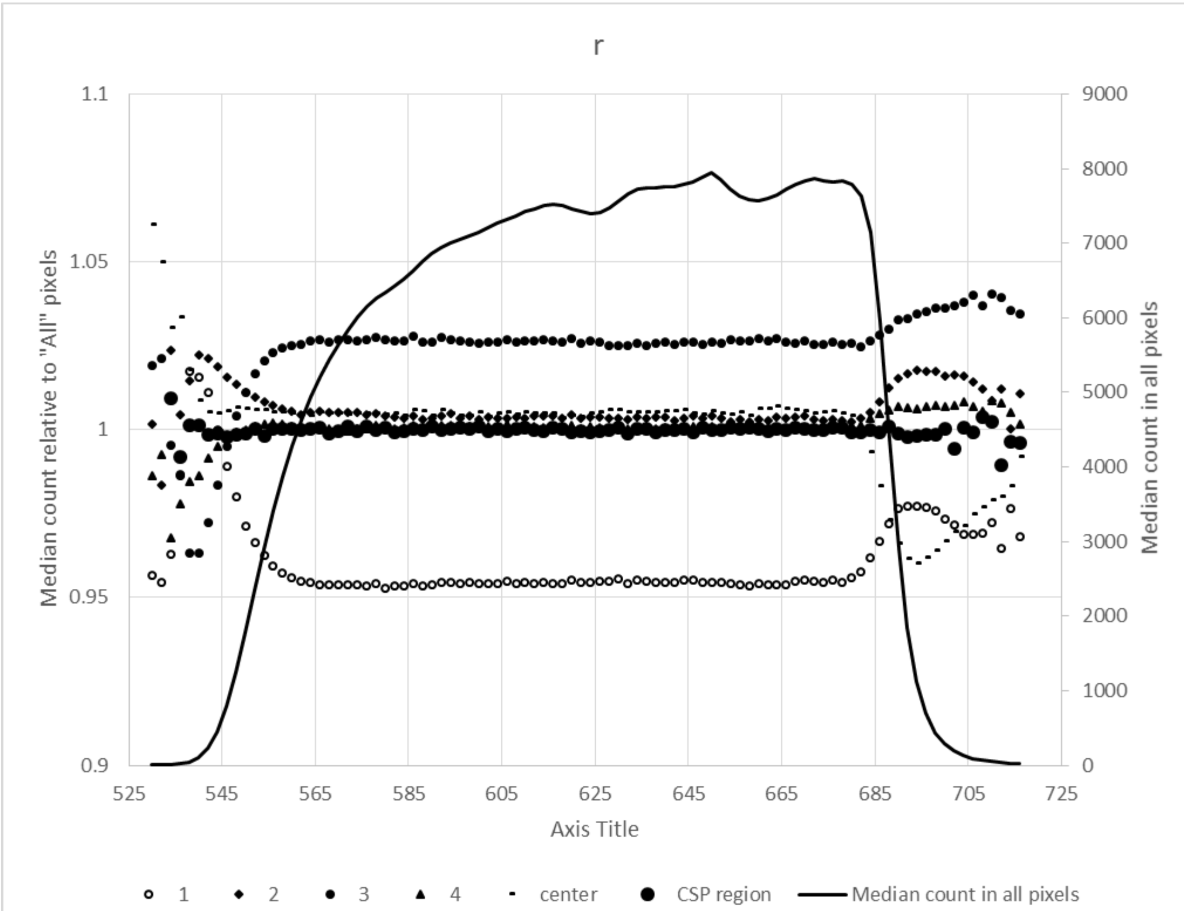

Figure 9: Spatial dependence vs. Wavelength for r filter

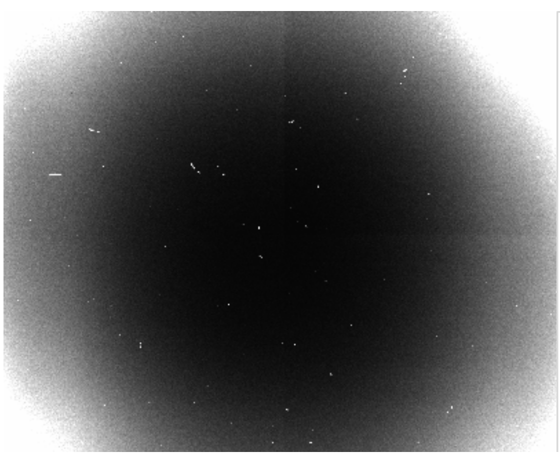

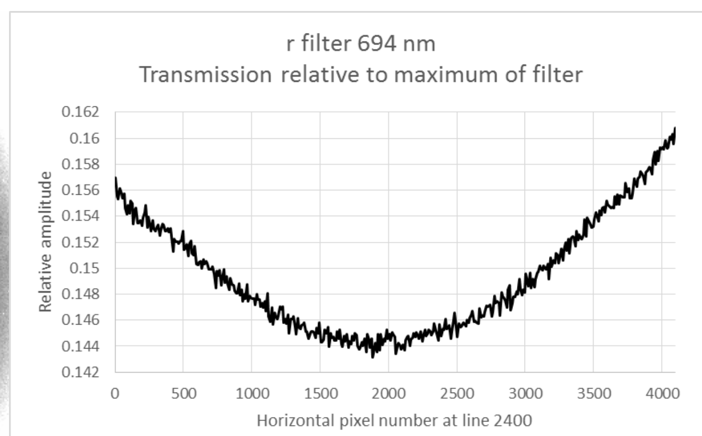

Figure 10a and 10b: (Left) CCD image at 694 nm with r filter, (Right) horizontal slice of the image at line 2400.

5. ERROR BUDGET

The tables 3 and 4 show the estimated measurement uncertainties for the 2 telescopes. The uncertainties are higher in the infrared in part because our light level is lower and also because the Germanium and InGaAs photodiodes are less sensitive than the Silicon photodiode.

Swope Estimated measurement error (All filters)	
Relative photodiode calibration uncertainty	1%
Relative photodiode noise level	0.03%
Relative noise level on CCD (in region)	0.05%
Total uncertainty (added in quadrature)	1%
Wavelength accuracy	0.1nm

Table 3: Swope estimated measurements error

DuPont Estimated measurement error		
Filter	Y	J, H
Transfer from dome flat screen to witness screen	1%	1%
Relative photodiode calibration uncertainty	2%	2%
Relative photodiode noise level	1%	2%
Relative drift level on camera image (in region)	1%	1%
Total uncertainty (added in quadrature)	2.7%	3.2%
Wavelength accuracy	2nm	2nm

Table 4: DuPont estimated measurements error

6. CONCLUSION:

We have measured the transmission function of the E2V camera on Swope from 300 to 1100nm in 6 different filters and with no filter present in the filter slot. We also measured the RetroCam camera on DuPont telescope from 900 nm to 1900nm in 3 filters. The results on the Swope have an excellent uncertainty of 1%. The DuPont results have a bigger uncertainty due to thermal drift and low light level but with the use of a witness screen and chopping of the signal before exposure, we were able to achieve an uncertainty of 3%. Each filter was scanned at least twice on at least 2 separate nights. The scans were performed with a wavelength step of 2nm on the Swope and 5nm on the DuPont

6.1 E2v CCD on Swope:

The new E2V CCD has a flatter response and is relatively more sensitive both in the red and the blue. The intrinsic response of the filters has not changed since Jan 2010, although the total throughput for each filter did change due to a change in the CCD QE. When looking at images from the whole CCD, there is up to a ~4% sensitivity dependence on the color and position of the pixel. A large part of this color dependence is due to the E2V CCD intrinsic non-uniformity and it is more pronounced below 400 nm and above 900nm. The filters also contribute to this effect, the strongest wavelength dependence is seen in filters where there is a sharp change in the transmission with wavelength. When restricting our use to a 500x500 pixel box in the center of Q3, the uniformity improves drastically and with the exception of the red edge of filters g and r, any variation with wavelength is much smaller than 1%.

6.2 RetroCam filters on DuPont:

The intrinsic response of the filters doesn’t appear to have changed since it was measured on the Swope in 2010. The small differences can be attributed in a difference of reflectivity between the Swope and DuPont mirrors.

ACKNOWLEDGEMENTS

Texas A&M University thanks Charles R. and Judith G. Munnerlyn, George P. and Cynthia W. Mitchell, and their families for support of astronomical instrumentation activities in the Department of Physics and Astronomy. Thanks also for the staff at Las Campanas Observatory for helping with the screen installation.

REFERENCES

[1] N. Kaiser et al., “Pan-STARRS: a large synoptic survey telescope array,” Proc. SPIE 4836, 154 (2002)
[2] Z. Ivezic et al., “LSST: from science drivers to reference design and anticipated data products,” arXiv:0805.2366 (2011)
[3] T. Abbott et al., “The Dark Energy Survey,” arXiv:astro-ph/0510346v1 (2005)
[4] Stubbs, Christopher W. et al, "Precise throughput determination of the PanSTARRS telescope and the gigapixel imager using a calibrated silicon photodiode and a tunable laser: initial results," ApJS, 191(2), 376-388 (2010).
[5] Rheault, J.-P. et al., “Spectrophotometric calibration system for DECam,” Proc. SPIE, 7735, 201 (2010)
[6] Rheault, J.-P. et al., “Spectrophotometric calibration system for DECam,” Proc. SPIE, 8446, 252 (2012)
[7] Stritzinger, Maximilian D., “The Carnegie Supernova Project: Second Photometry Data Release of Low-redshift Type Ia Supernovae,” AJ, 142(5), 156 (2011)